Comparison of Induction and PM Synchronous Motor Drives for EV Application Including Design Examples

Gianmario Pellegrino, *Member, IEEE*, Alfredo Vagati, *Fellow, IEEE*, Barbara Boazzo, and Paolo Guglielmi, *Member, IEEE*

***Abstract*—Three different motor drives for electric traction are compared, in terms of output power and efficiency at the same stack dimensions and inverter size. Induction motor (IM), surface-mounted permanent-magnet (PM) (SPM), and interior PM (IPM) synchronous motor drives are investigated, with reference to a common vehicle specification. The IM is penalized by the cage loss, but it is less expensive and inherently safe in case of inverter unwilled turnoff due to natural de-excitation. The SPM motor has a simple construction and shorter end connections, but it is penalized by eddy-current loss at high speed, has a very limited transient overload power, and has a high uncontrolled generator voltage. The IPM motor shows the better performance compromise, but it might be more complicated to be manufactured. Analytical relationships are first introduced and then validated on three example designs and finite element calculated, accounting for core saturation, harmonic losses, the effects of skewing, and operating temperature. The merits and limitations of the three solutions are quantified comprehensively and summarized by the calculation of the energy consumption over the standard New European Driving Cycle.**

***Index Terms*—Electric machine design comparison, induction motor (IM) drives, permanent-magnet (PM) machines, synchronous motor drives, traction motor drives, variable-speed drives.**

I. Introduction

STATE-OF-THE-ART drive trains for electric vehicles (EVs) are often equipped with induction motors (IMs) or permanent-magnet (PM) synchronous motors [1], [2]. IM drives are adopted for their ruggedness and universal availability. Also, on the control side, field-oriented vector control of IMs is considered a standard, industrially. Moreover, IMs are naturally de-excited in case of inverter fault, and this is very welcome among car manufacturers, for safety reasons.

PM motor drives are considered to have a higher torque density and efficiency, with respect to IMs. Among PM motors, both surface-mounted PM (SPM) and interior PM (IPM) types are adopted for traction [3]. SPM motors for traction have concentrated stator coils [4], i.e., very short end connections and an easier stator construction. They suffer from eddy-current loss in the PMs at high speed and need structural sleeves for PM retention. Arc magnets such as the ones in Fig. 1(c) can be a problem industrialwise, but different rotor solutions are possible, also contributing to mitigate PM loss [18]. IPM motors require rotors with multiple flux barriers for having a high saliency, such as the one in Fig. 1(b), which might look complicated industrialwise. However, the high saliency is synonymous of a much larger overload torque over the entire speed range [5], a safer back electromotive force in uncontrolled generator operation [6], and little sensitivity to PM temperature.

Synchronous PM drives of both types require a custom control algorithm when flux-weakening operation is required over a wide speed range, as it is the case of traction. The motor magnetic model must be consistently identified for accurate control with the experimental identification tests that are considered cumbersome if compared to the standard ones that are usual for IMs. The recent issue of the rare-earth magnet price volatility is seriously questioning the adoption of PM motor drives [7]. In this scenario, multilayer IPM motors are more suitable for replacing the rare-earth magnets with cheaper ferrite magnets, at least in some cases [9], while SPM and single-layer IPMs are not.

The comparison between IM, SPM, and IPM motor drives for EVs is proposed, at a given vehicle specification and with the three motors having the same outer dimensions of the active parts (stack diameter and length) and the same inverter size (maximum voltage and current). This paper extends the comparison in [5] to include the asynchronous motor, giving further insights on aspects such as skewing and PM temperature.

Three example motors are designed and finite element analysis (FEA) characterized. Their laminations are represented in Fig. 1. Unfortunately, it was not possible to build and test three prototypes to be experimentally compared. However, finite-element simulation can still be considered a consistent instrument of virtual prototyping of electrical machines, accepted industrialwise, as documented in the literature [12], [20], [21], and also for loss evaluation [22].

II. Terms of the Comparison

A. Vehicle Specification

As summarized in Fig. 2, EVs require a constant-torque operating region at low speed for starting and uphill march and,

Manuscript received January 18, 2012; revised June 5, 2012; accepted June 9, 2012. Date of publication November 16, 2012; date of current version December 31, 2012. Paper 2011-EMC-610.R1, approved for publication in the IEEE Transactions on Industry Applications by the Electric Machines Committee of the IEEE Industry Applications Society.

The authors are with the Politecnico di Torino, 10129 Turin, Italy (e-mail: gianmario.pellegrino@polito.it; Alfredo.Vagati@polito.it; barbara.boazzo@polito.it; paolo.guglielmi@polito.it).

Color versions of one or more of the figures in this paper are available online at http://ieeexplore.ieee.org.

Digital Object Identifier 10.1109/TIA.2012.2227092

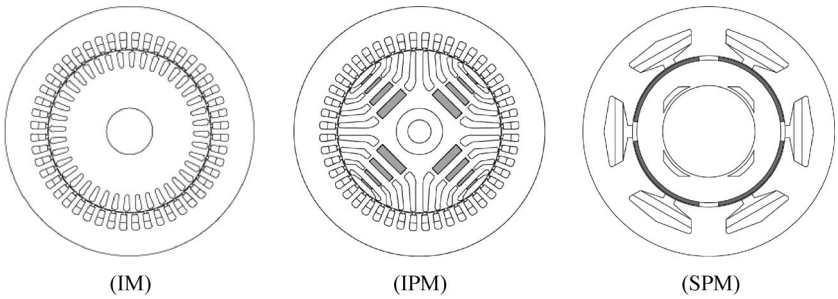

Fig. 1. IM, IPM motor, and SPM motor under investigation.

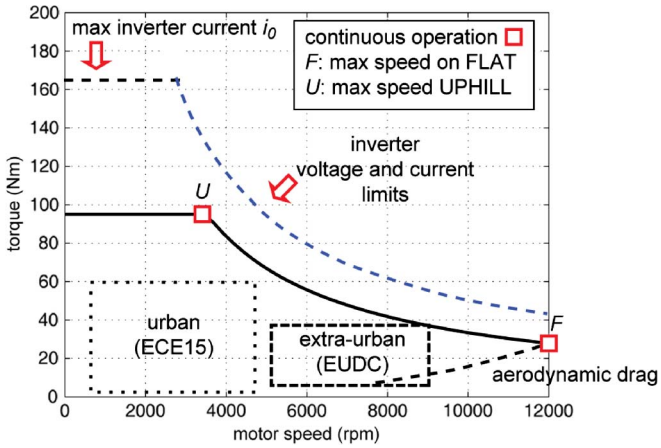

Fig. 2. Example of target specification for an EV.

then, a constant power speed range at higher vehicle speed. The continuous power at maximum speed P_1 determines the maximum speed of the vehicle on flat (***F*** red square, for *Flat*). The continuous stall torque T_1 determines the maximum slope that the vehicle can climb continuously (***U*** red square, for *Uphill*). Transient overload torque and power are limited by the inverter current rating (i_0), and the combination of voltage and current limits (v_0, i_0), respectively. The typical areas of urban and extra-urban operations are also evidenced in Fig. 2, which will be calculated according to the New European Driving Cycle New European Driving Cycle for the final designs of Section VII. ECE15 and EUDC in Fig. 2 indicate urban and extra urban, according to the NEDC standard [23]. Detailed vehicle specifications are reported in the Appendix.

B. Common Data and Goals of the Comparison

The torque versus speed profiles of Fig. 2 are indicative but not mandatory, except for point F. The three drives under comparison must comply with ***the basic requirement of giving the same maximum vehicle speed***, i.e., giving the same continuous power at the maximum motor speed of 12 000 r/min. All the other parameters evidenced in Fig. 2 are matter of the comparison: continuous torque at point U, maximum overload torque at given inverter current, transient overload, and efficiency over the whole operation area and in the preferred maximum efficiency area. The stack outside diameter, stack length, and air-gap length are the same for the three motors, as well as the same liquid cooling setup. It is assumed that the stator windings are at 130 °C in continuous operation, the PMs are at 150 °C, and the rotor of the IM is at 180 °C. The inverter voltage and current are set to $v_0 = 173$ Vpk phase voltage, corresponding to a 300 V dc link, and $i_0 = 360$ Apk phase current.

III. IM Drive

A. Motor Model in the Rotor Field-Oriented Frame

The dq reference frame, synchronous to the rotor flux, is considered. In this frame, the stator flux vector components, at steady state, become

$$\begin{cases} \lambda_{sd} = L_s \cdot i_{sd} \\ \lambda_{sq} = \sigma \cdot L_s \cdot i_{sq} \end{cases} \tag{1}$$

where L_s is the stator self-inductance, σ is the total leakage factor (2), and σL_s is the stator transient inductance

$$\sigma = 1 - \frac{L_M^2}{L_s \cdot L_r}. \tag{2}$$

The steady-state expressions of stator voltage and torque are

$$\bar{v}_{sdq} = R_s \cdot \bar{i}_{sdq} + j\omega \cdot \bar{\lambda}_{sdq} \tag{3}$$

$$T = \frac{3}{2} \cdot p \cdot (\bar{\lambda}_{sdq} \wedge \bar{i}_{sdq}) \tag{4}$$

where ω is the synchronous electrical speed. Last, the slip speed at steady state is

$$\omega_{sl} = \tau_r^{-1} \cdot \left(\frac{i_{sq}}{i_{sd}} \right) \tag{5}$$

where $\tau_r = L_r / R_r$ is the rotor time constant and R_r is the rotor resistance reported to the stator. Independently of the control technique (rotor-field-oriented, stator-field-oriented, direct torque control), the magnetic model (1) can be used in association to (3)–(5) for describing the torque and power curves as a function of rotor speed, at given voltage and current limits [15], [16].

B. Power Curves at Constant Current

The stator current and flux linkage vectors will be indicated, from now on, as flux linkage and current, with no subscript s,